Materials Research. 2019; 22(suppl. 1): e20180849
DOI: http://dx.doi.org/10.1590/1980-5373-MR-2018-0849

Microstructure and Thermal Analyses of $Cu_{87-x}Al_{13}Nb_x$ High-Temperature Shape Memory Alloys

***Jackson de Brito Simões*[a]*, *Endira Maria Araújo Pereira*[b], *José Joelson de Melo Santiago*[b], *Carlos José de Araújo*[b]**

[a]*Departmento de Engenharia Mecânica, Universidade Federal Rural do Semi-Arido (UFERSA), RN 233, km 01, Sítio Esperança II, Zona Rural, 59780-000, Caraúbas, RN, Brasil.*
[b]*Departmento de Engenharia Mecânica, Universidade Federal de Campina Grande (UFCG), Av. Aprígio Veloso, 882, Bairro Universitário, 58429-140, Campina Grande, PB, Brasil.*

Received: December 11, 2018; Revised: July 24, 2019; Accepted: October 24, 2019

This paper presents a thermal and microstructural characterization of $Cu_{87-x}Al_{13}Nb_x$ (wt%) high temperature shape memory alloys (HTSMA), with Nb contents ranging from 1 to 3%. The alloys were obtained by arc melting under argon atmosphere. Thermal characterization was performed by differential scanning calorimetry (DSC), revealing that the phase martensitic transformation of all the studied alloys occurs in the range of 200 ºC to 450 ºC. Thermal cycling in this temperature range caused the martensitic transformation to disappear after approximately 6 cycles. However, a new heat treatment at 850 ºC followed by water quenching causes the martensitic transformation to be recovered. Microstructural characterization was performed using optical microscopy (OM) and scanning electron microscopy (SEM), revealing the presence of Nb precipitates in a Cu-Al martensitic matrix, mainly in the Nb-rich compositions. These different microstructures with Nb particles cause a hardness variation that initially decreases between 0.5 %Nb (275HV) and 1.0 %Nb (225HV), then increasing continuously up to 3.0% Nb (380HV).

Keywords: *Cu-Al-Nb alloys, high-temperature shape memory alloys, phase martensitic transformation, temperatures, shape memory alloy.*

1. Introduction

Shape memory alloys (SMA) are attractive materials due to the smart properties of shape memory effect (SME) and superelasticity (SE), which enable SMA to be widely applied in industry and medical areas [1-4]. Owing to all phenomena associated with SMA, these materials can be used as sensors and actuators [2, 3, 5].

Most commercial SMA products are restricted to near room-temperature usage because they largely consist of alloys with martensitic transformation temperatures lower than 150 °C [5-9]. These SMA are not suitable for use in high-temperature applications such as rocket fuels and automobile engines. Considering that there is a demand for the production of high-temperature shape memory alloys (HTSMA) [3, 10, 11], some research works have been performed to allow the use of SMA in high temperature conditions, mainly through modifications in chemical composition [12-15].

Cu-based and NiTi alloys are important groups of SMA. Due to the superior combination of physical and mechanical properties of NiTi based alloys (low density, high tensile strength, corrosion resistance, biocompatibility, damping and recoverable strain of up to 8%), these compositions have received more attention for the development of HTSMA[9, 10]. Addition of Zr, Hf, Pd and Pt to the NiTi binary system tend to increase martensitic transformation temperatures [5, 11, 16, 17]. Others HTSMA possibilities include Cu-Al based alloys, such as Cu–Al–Nb alloys [18-20]. The addition of Nb to Cu–Al alloys causes the formation of a large number of primary particles identified as $Nb(Cu, Al)_2$ and Nb(Cu, Al) [2, 6, 20]. In general, these alloys exhibit martensitic transformation start temperature (M_s) higher than 200 °C [2, 6, 7, 20, 21].

Cu-based SMA are known for their easy production and application possibilities, in addition to lower costs in comparison to NiTi alloys [1, 10, 14 20, 22, 23]. The base for these alloys are generally binary systems such as Cu–Zn, Cu–Al and Cu–Sn. Among these, Cu–Sn does not show good thermoelastic transformation, while Cu–Sn has rather limited application due its brittleness. The potential uses and properties can be improved by the addition of Al, Si and Sn to Cu–Zn alloys and by the addition of Ni, Be, Zn and Mn to Cu–Al alloys [22].

Furthermore, there is an increasing need to develop SMA parts that can be used over a large temperature range (lower and higher than 200 ºC) due to the requirements of engineering applications such as automotive, robotics, power generation and aerospace industries [12, 24]. Therefore, researches are being carried out for the development of SMA that have martensitic transformation start temperature (M_s) higher than 200 ºC, making these alloys suitable for high temperatures environments [25]

* e-mail: eng_jacksonsimoes@hotmail.com

As mentioned above, Nb addition in Cu-Al alloys causes an increase in martensitic transformation temperatures. This element is virtually insoluble in copper matrix, causing segregation of primary phases. SME at temperatures above 350 °C is a feature of some compositions of these alloys, as reported by Lelatko and Morawiec [20]. Therefore, the aim of this work is to obtain Cu-Al-Nb HTSMA using an arc melting process, as well as to verify its thermal stability from 200 °C to 450 °C. There is also an interest in evaluating microstructure and the influence of Nb content on thermal and hardness behaviors of these Cu-Al-Nb HTSMA.

2. Experimental Procedures

Six buttons with nominal compositions $Cu_{87-x}Al_{13}$-Nb_x (x = 0.5, 1.0, 1.5, 2.0, 2.5 and 3.0 wt%) were obtained by arc melting in a process called Plasma Skull Push Pull (PSPP), as described by De Araujo et al [26]. In this process, the Cu, Al and Nb pure metals are melted and remelted five times to ensure homogeneity, under argon atmosphere in a copper crucible. Thereafter, the buttons were remelted one last time in an induction melting machine with injection by centrifugation (Powercast 1700, EDG) into a ceramic mold (heated at 750 °C) to obtain the final specimens. All as-cast Cu-Al-Nb alloy compositions were heat treated at 850 °C for 20 minutes, followed by water quenching at room temperature.

All specimens for microstructure examination were prepared by standard metallographic procedures followed by etching in a solution of iron chloride. Microstructures were observed using optical microscopy (OM) (model BX51M, OLYMPUS) and scanning electron microscopy (SEM) (model VEGA 3SBH, TESCAN) operated at 20 kV.

Martensitic transformation temperatures were determined by differential scanning calorimetry (DSC) (Q20 model, TA Instruments) at a rate of 10 °C.min^{-1} for both heating and cooling in the temperature range from 200 to 450 °C. Additionally, a thermal cycling with ten cycles in the test temperature range was performed to verify the phase martensitic transformation stability of the Cu-Al-Nb HTSMA.

Vickers microhardness (HV) measurements were carried out using a model FM-700 Future-Tech equipment. Indentations were performed applying 3N for 10 seconds. HV values are an average of at least 10 indentations for each alloy composition, excluding the lowest and highest values.

3. Results and Discussion

3.1 Thermal analysis

DSC analysis of the as-cast Cu-Al-Nb HTSMA samples revealed no martensitic transformation peaks. Thus, alloys were subjected to a solution heat treatment (850 °C for 20 minutes) followed by water quenching at room temperature. After heat treatment, new DSC tests were performed showing the presence of the martensitic phase transformation peaks in all Cu-Al-Nb HTSMA compositions. Figure 1 shows DSC cooling and heating curves for the $Cu_{86}Al_{13}Nb_1$ HTSMA. Table 1 summarizes martensitic transformation temperatures for each composition. Start and finish martensitic transformation temperatures were determined from the intersection of tangent lines in the DSC peaks, as pointed out in Figure 1.

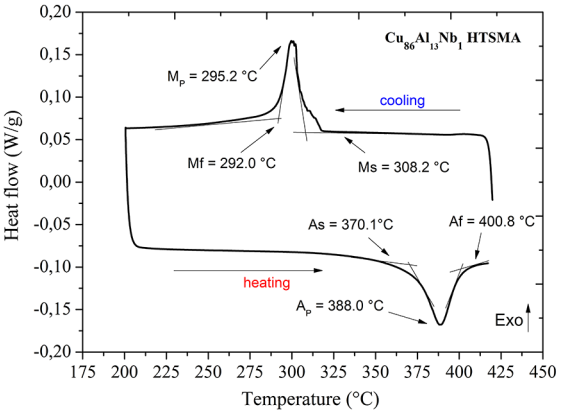

Figure 1. Martensitic transformation temperatures of the $Cu_{86}Al_{13}Nb_1$ HTSMA obtained by DSC.

For heating, as final martensitic transformation temperatures (A_f) are very high, close to temperatures of annealing heat treatments (between 400 and 500 °C), ten thermal cycles were performed to verify the phase martensitic transformation stability of these Cu-Al-Nb HTSMA. Figure 2 shows that after each cycle, the martensitic transformation enthalpy continuously decreases, leading to the disappearance of martensitic transformation peaks from the sixth cycle. This behavior was verified for all alloy compositions. Lelatko et al.[2] observed a very similar behavior for a Cu-Al-Nb HTSMA with 2.5 %Nb, observing that the martensitic transformation is reversible only for the first five cycles.

Table 1. Martensitic transformation temperatures and thermal hysteresis of the Cu-Al-Nb HTSMA samples.

Nb (wt%)	M_f (°C)	M_s (°C)	A_s (°C)	A_f (°C)	Hysteresis (°C)
0.5%	292.1	298.2	371.0	407.8	92.8
1.0%	292.2	308.2	370.1	400.8	87.2
1.5%	283.5	309.2	368.6	394.9	88.6
2.0%	267.7	299.3	362.2	395.3	89.1
2.5%	260.5	283.0	356.2	403.5	107.7
3.0%	235.7	292.4	342.3	408.5	128.0

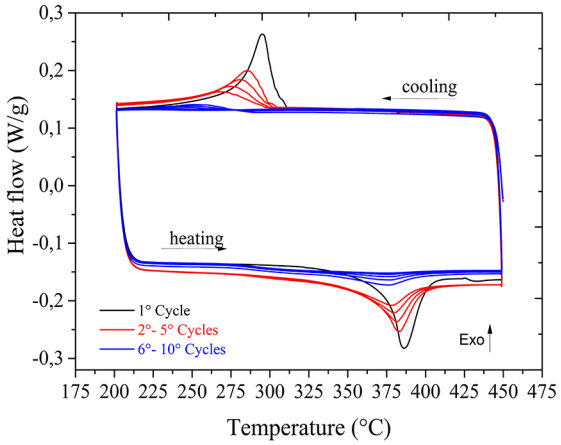

Figure 2. Thermal cycling effect in the $Cu_{86}Al_{13}Nb_1$ HTSMA.

To verify the possibility of restoring the phase martensitic transformation hindered after ten thermal cycles (Figure 2), each Cu-Al-Nb HTSMA sample was resubmitted to the solution heat treatment followed by water quench. Figure 3 shows that in all studied Cu-Al-Nb HTSMA compositions present the reversible phase martensitic transformation after this second heat treatment, even after the 10 thermal cycles. This behavior suggests that the alloys can be used again for some thermal cycles and consequently promote the ability to perform mechanical work in some applications. It is noteworthy that in all cases the martensitic transformation temperatures, as well as the thermal hysteresis, were approximately the same for all Nb contents, as shown in Figure 3 and Table 2. Thermal hysteresis was measured as the difference between the peak martensitic transformation temperatures austenite (A_p) and martensite (M_p).

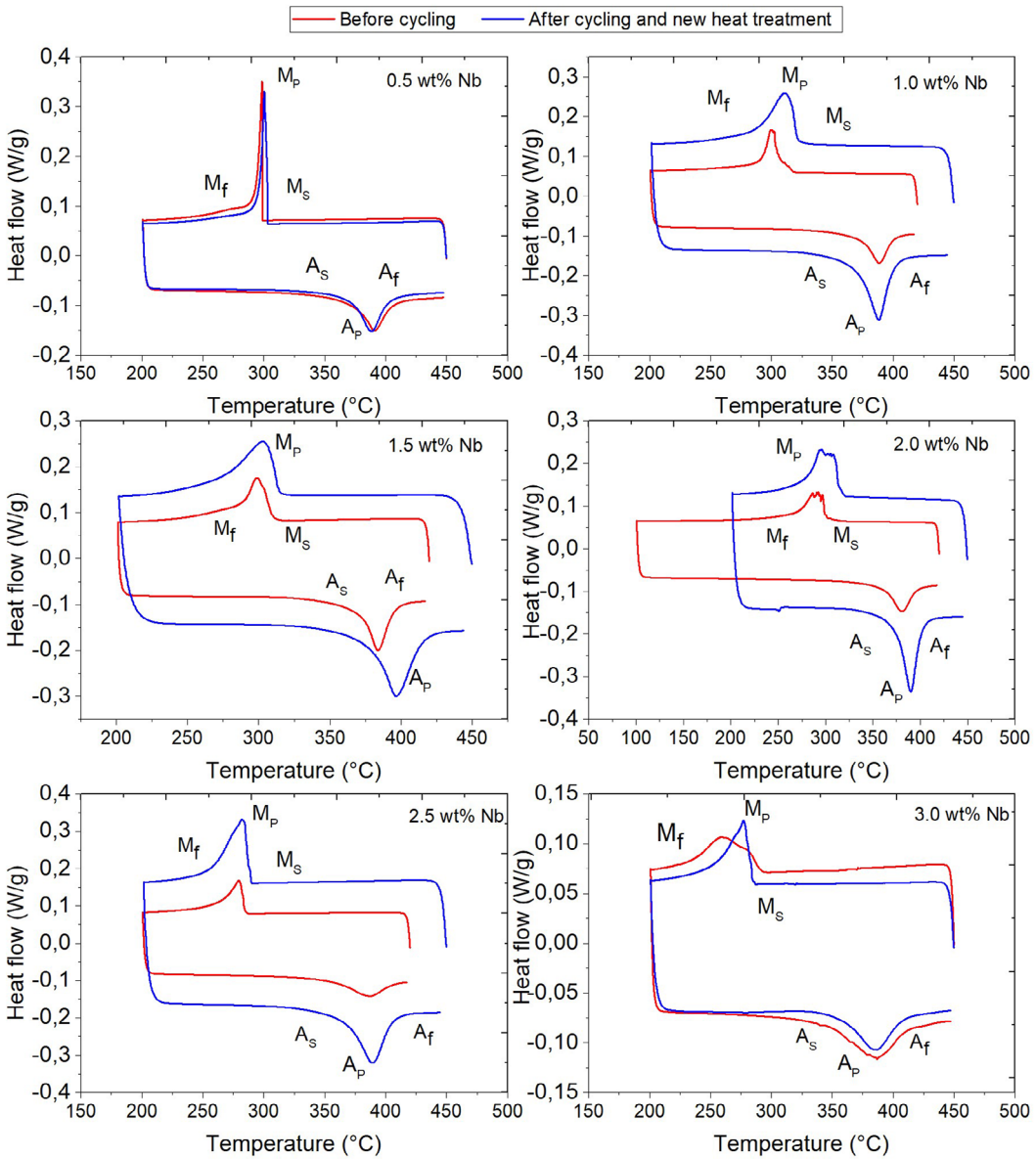

Figure 3. Superposition of DSC results before and after thermal cycling with phase martensitic transformation restoration through heat treatment for all Cu-Al-Nb HTSMA samples.

Table 2. Martensitic transformation temperatures and thermal hysteresis of the Cu-Al-Nb HTSMA samples after post cycling with later re-quenching.

Nb (wt%)	M_f (°C)	M_s (°C)	A_s (°C)	A_f (°C)	Hysteresis (°C)
0.5%	295.3	302.5	371.7	399.0	88.5
1.0%	290.6	321.3	365.5	403.8	77.0
1.5%	267.7	315.2	373.4	416.8	95.5
2.0%	278.7	314.2	367.7	402.2	95.8
2.5%	258.2	288.1	365.2	406.2	105.9
3.0%	254.1	284.6	356.3	406.8	108.6

Concerning martensitic transformation temperatures, according to Lelatko et al.[2], Nb is a practically insoluble element in the copper matrix, which causes a primary phase segregation in the Cu-Al-Nb alloys. This originates an increase in martensitic transformation temperatures in relation to the Cu-Al system. It can be seen that both M_s and A_f values do not vary significantly. Moreover, the martensitic transformation characteristics of the $Cu_{87-x}Al_{13}Nb_x$ alloys (x = 0.5, 1.0, 1.5, 2.0, 2.5 and 3.0 wt% Nb) coincides with that of the first type thermal transformation described by Liu and Mu[2] because of $A_f > A_s > M_s > M_f$.

Additionally, as can be verified in Tab. 2, Nb promotes an increase in the thermal hysteresis from mean values close to 90 °C for the range of 0.5 – 2.0 %Nb, to 128 °C for 3.0 %Nb.

3.2 Microstructure analysis

Figure 4 show optical micrographs of the $Cu_{87-x}Al_{13}Nb_x$ HTSMA studied alloys (x = 0.5, 1.0, 1.5, 2.0, 2.5 and 3.0 wt% Nb) after the heat treatment described in section 3.1. Increasing the Nb content (insoluble in the copper matrix) gives rise to structures that most likely are precipitates that might be caused by the segregation of the primary phases, probably $Nb(Cu, Al)_2$ (coarse) and Nb(Cu, Al) (fine) as predicted by Lelatko et al. [2,20].

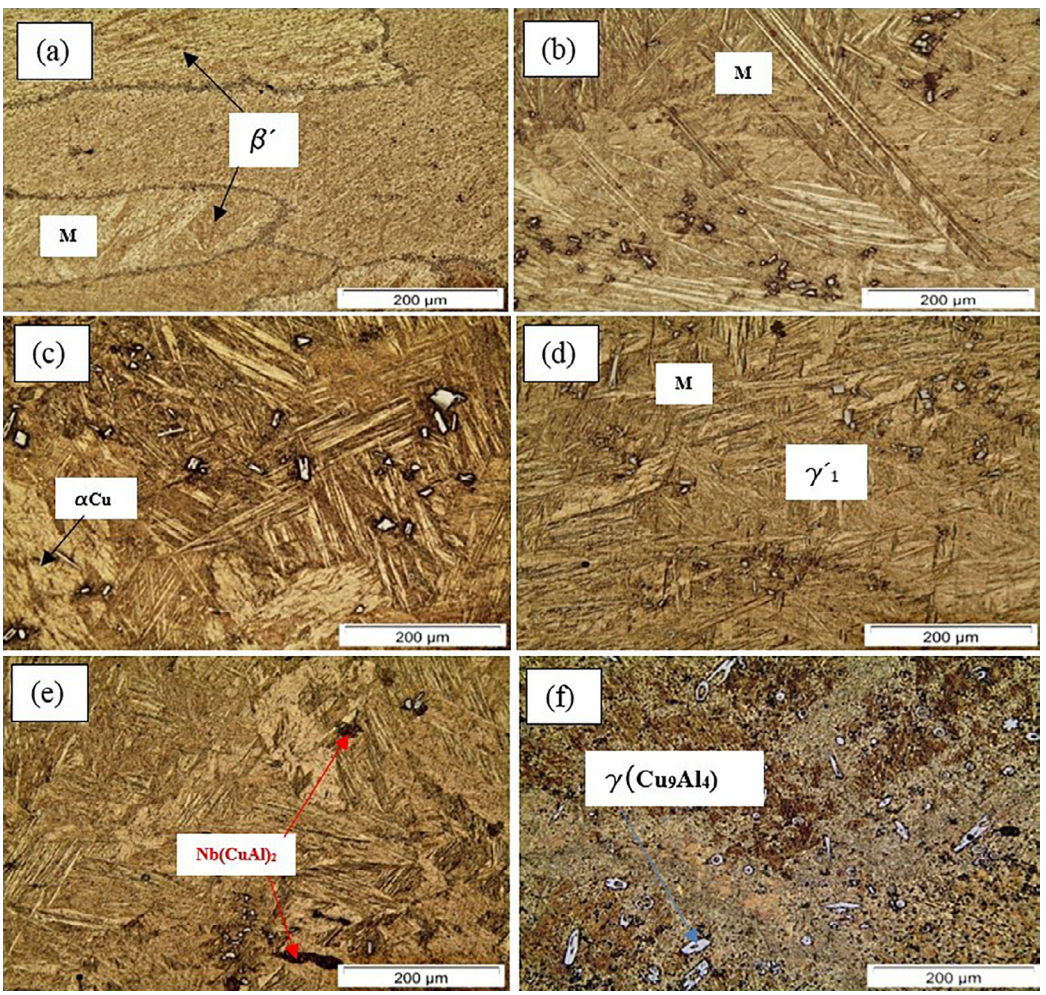

Figure 4. OM images revealing fine and coarse martensite as well as precipitate particles in the microstructure of the Cu-Al-Nb alloys. (a) 0.5 %Nb; (b) 1.0 %Nb; (c) 1.5 %Nb; (d) 2.0 %Nb; (e) 2.5 %Nb; (f) 3.0 %Nb.

The regions closest to these particles serve as nuclei for the appearance of martensite variants with multiple orientations, as can be seen in Figs. 4(b-e). Two martensite structures typically produced are thin β'_1 type (18R) and thick γ'_1 type (2H). It is seen from Figure 4 that the predominant β'_1 type thin martensite is observed for $x = 0.5$ (Figure 4a), but the γ'_1 type martensite that is thicker compared to β'_1 type thin martensite is present for $x > 1$ (Figure 4d).

SEM images from Figure 5 confirm the formation of Nb precipitates observed by OM. For the alloy with 0.5 %Nb, a uniform distribution of very fine particles along the alloy microstructure is verified. With the increase in Nb content, these particles become larger in size and more grouped, i.e., there is a non-uniform distribution along the microstructure. According to Lelatko et al [6], the particles of these phases present inside the martensite microstructure create additional stress fields. When the particles are large, internal surfaces between particles and martensite plates are the most favorable regions for nucleation of thin martensite variants with another orientation.

The low thermal stability observed in Figure 2 is probably due to intense diffusion process at high temperatures during repeated cooling and heating cycles [6]. The presence of these Nb rich particles in the Cu-Al matrix causes an increase in the martensitic transformation temperatures to values higher than 250 °C, comparing to the ternary Cu-Al-Ni alloys [20]. In addition, the increase in content of primary particles leads to an increase of the thermal hysteresis (approximately 90 °C to 128 °C).

To identify chemical composition of the precipitate particles, which are possibly Nb precipitates, a semi quantitative analysis was performed by EDS in all Cu-Al-Nb HTSMA samples. The EDS results are shown in Figure 6. Also based on the works of Lelatko et al [6, 18-20], probably these phases are of two types, namely $Nb(Cu, Al)_2$ and Nb(Cu, Al).

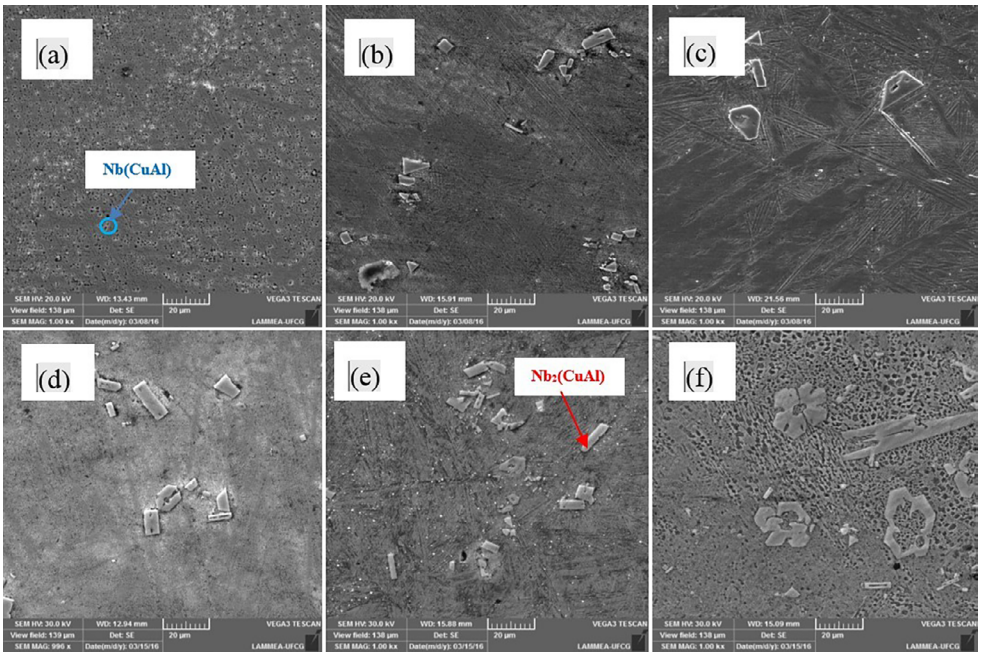

Figure 5. SEM images revealing precipitate particles with 1000x magnification. Numbers indicate the Nb content in wt%.

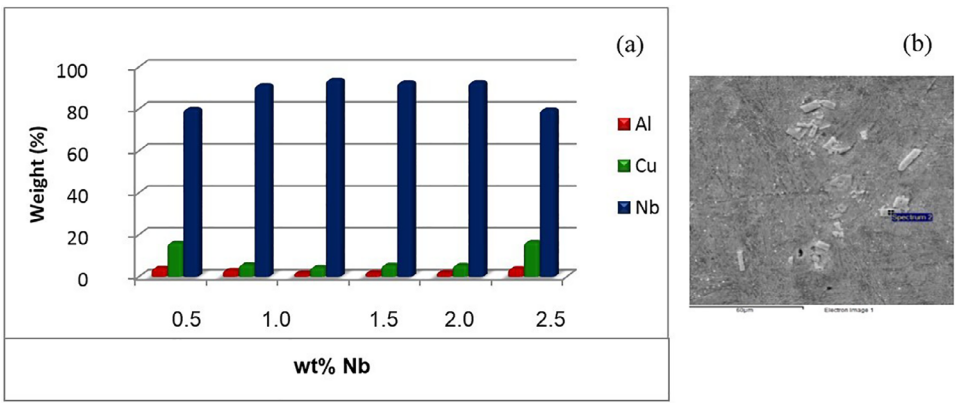

Figure 6. EDS analysis of some particles observed in the matrix of Cu-Al-Nb HTSMA. (a) Graph of chemical composition of the samples by means of point analysis. (b) $Nb_2(CuAl)$ precipitate particles.

3.3 Mechanical behavior – Hardness

Vickers hardness profile of the Cu-Al-Nb HTSMA samples as a function of Nb content is shown in Figure 7. Nb has a significant influence on the hardness of the material, contrary to the behavior observed by Lelatko et al [6]. For the $Cu_{86.5}Al_{13}Nb_{0.5}$ HTSMA, the average value of hardness was 352 HV, which might be associated with the uniform distribution of fine primary particles of Nb in the Cu-Al matrix. Figure 7 shows a hardness reduction followed by an increase from Cu-Al-Nb HTSMA samples with 1.0 %Nb (225 HV), reaching 275 HV to 2.5 %Nb and 380 HV to 3.0 %Nb. This behavior might be associated with a greater dispersion and increase of dimensions of the primary Nb particles. It should be noted that average values of the order of 400 HV have already been reported for Cu-Al-Nb alloys (2% Nb) containing small additions of Ti (0.3%) and B (0.05%)[18].

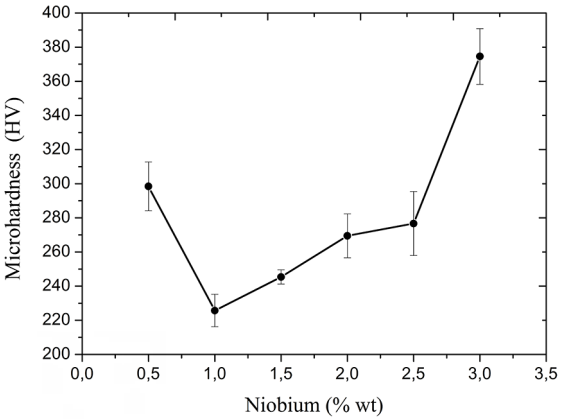

Figure 7. Microhardness (HV) behavior of the Cu-Al-Nb HTSMA as a function of Nb content.

4. Conclusions

In this work the feasibility of obtaining Cu-Al-Nb HTSMA by arc melting with argon protective atmosphere, called PSPP process[26], was demonstrated. Most of the works found in the literature use magnetic induction melting.

It was found that the replacing Cu content with Nb in the $Cu_{87-x}Al_{13}$-Nb_x (wt%) system caused the phase martensitic transformation to occur in the range of approximately 250 °C (M_f) to 400 °C (A_f), for all compositions evaluated. Thermal cycling in this temperature range revealed that the phase martensitic transformation disappears after approximately six heating and cooling cycles. However, a further heat treatment at 850 °C for 20 minutes followed by water quenching at room temperature restores phase martensitic transformation within essentially the same temperature range and thermal hysteresis. Thus, it was shown that the material functional properties related to martensitic phase martensitic transformation in these alloys can be recovered after an initial use in the considered high temperature range, higher than 200 °C.

It has been found that the microstructures of studied Cu-Al-Nb HTSMA vary substantially with the Nb content, resulting in Nb-rich particles in a matrix of martensite variants. This microstructure leads to a hardness behavior that initially decreases between 0.5 %Nb (275 HV) and 1.0 %Nb (225 HV) followed by a continuous increase up to 380 HV to 3 %Nb.

5. Acknowledgements

The authors would like to thank UFERSA by the technical cooperation agreement N° 07/2017 23091.005950/2017-19, project grant PEG00001-2017 and PEG20001-2018. Also CNPq Brazilian research agency for funding the following projects: National Institute of Science and Technology - Smart Structures in Engineering (Grant 574001/2008-5), Universal 14/2016 (Grant 401128/2016-4) and PQ-1C (Grant 304658/2014-6).

6. Reference

1. Otsuka K, Wayman CM, eds. *Shape Memory Materials*. 1st ed. Cambridge: Cambridge University Press; 1998.

2. Liu C, Mu HW. Martensitic transformation and shape memory recovery property of $Cu_{72}Al_{26.5}Nb_{1.5}$ high temperature shape memory alloy. *Journal of Alloys and Compounds*. 2010;508(2):329-332.

3. Lagoudas DC, ed. *Shape Memory Alloys: Modeling and Engineering Applications*. New York: Springer Verlag US; 2008.

4. Firstov GS, van Humbeeck J, Koval YN. High Temperature Shape Memory Alloys Problems and Prospects. *Journal of Intelligent Material Systems and Structures*. 2006;17(12):1041-1047.

5. Karaca HE, Acar E, Tobe H, Saghaian SM. NiTiHf-based shape memory alloys. *Materials Science and Technology*. 2014;30(13 Pt A/B):1530-1544.

6. Lelatko J, Morawiec N, Koval YN, Kolomyttsev VI. Structure and properties of high-temperature alloys with the effect of shape memory in the system Cu−Al−Nb. *Metal Science and Heat Treatment*. 1999;41(8):351-353.

7. Font J, Cesari E, Muntasell J, Pons J. Thermomechanical cycling in Cu–Al–Ni-based melt-spun shape-memory ribbons. *Materials Science and Engineering: A*. 2003;354(1):207-211.

8. Hsu DHD, Hornbuckle BC, Valderrama B, Barrie F, Henderson HB, Thompson GB, et al. The effect of aluminum additions on the thermal, microstructural, and mechanical behavior of NiTiHf shape memory alloys. *Journal of Alloys and Compounds*. 2015;638:67-76.

9. Rehman SU, Khan M, Khan AN, Jaffery SHI, Ali L, Mubashar A. Improvement in the Mechanical Properties of High Temperature Shape Memory Alloy ($Ti_{50}Ni_{25}Pd_{25}$) by Copper Addition. *Advances in Materials Science and Engineering*. 2015;2015:434923.

10. Lexcellent C. *Shape-Memory Alloys Handbook*. 1st ed. Hoboken: John Wiley & Sons; 2013.

11. Saghaian SM, Karaca HE, Tobe H, Souri M, Noebe R, Chumlyakov YI. Effects of aging on the shape memory behavior of Ni-rich $Ni_{50.3}Ti_{29.7}Hf_{20}$ single crystals. *Acta Materialia*. 2015;87:128-141.

12. Qader IN, Kök M, Dağdelen F. Effect of heat treatment on thermodynamics parameters, crystal and microstructure of (Cu-Al-Ni-Hf) shape memory alloy. *Physica B: Condensed Matter*. 2019;553:1-5.

13. Jani JM, Leary M, Subic A, Gibson MA. A review of shape memory alloy research, applications and opportunities. *Materials & Design (1980-2015)*. 2014;56:1078-1113.

14. de Araújo APM, Simões JB, Araújo CJ. Analysis of Compositional Modification of Commercial Aluminum Bronzes to Obtain Functional Shape Memory Properties. *Materials Research*. 2017;20(Suppl 2):331-341.

15. Chen J, Li Z, Zhao YY. A high-working-temperature CuAlMnZr shape memory alloy. *Journal of Alloys and Compounds*. 2009;480(2):481-484.

16. Patriarca L, Sehitoglu H. High-temperature superelasticity of $Ni_{50.6}Ti_{24.4}Hf_{25.0}$ shape memory alloy. *Scripta Materialia*. 2015;101:12-15.

17. Potapov PL, Shelyakov AV, Gulyaev AA, Svistunov EL, Matveeva NM, Hodgson D. Effect of Hf on the structure of Ni-Ti martensitic alloys. *Materials Letters*. 1997;32(4):247-250.

18. Lelatko J, Morawiec H. The effect of Ni, Co and Cr on the primary particle structure in Cu–Al–Nb–X shape memory alloys. *Materials Chemistry and Physics*. 2003;81(2-3):472-475.

19. Lelatko J, Morawiec H. The modeling of the deformation behavior of Cu–Al–Nb–X shape memory alloys containing primary particles. *Materials Science and Engineering: A*. 2008;481-482:684-687.

20. Lelatko J, Morawiec H. High temperature Cu-AI-Nb- based shape memory alloys. *Journal de Physique IV (France)*. 2001;11(PR8):487-492.

21. Gong SK, Ma YQ, Jiang CB, Xu HB. Effect of Heat Treatment on Transformation Behavior in CuAlNb Shape-Memory Alloys with High Transformation Temperatures. *Materials Science Forum*. 2001;394-395:383-386.

22. Duerig TW, Albrecht J, Gessinger GH. A Shape-Memory Alloy for High-Temperature Applications. *JOM*. 1982;34(12):14-20.

23. Sathish S, Mallik US, Raju TN. Microstructure and Shape Memory Effect of Cu-Zn-Ni Shape Memory Alloys. *Journal of Minerals and Materials Characterization and Engineering*. 2014;2(2):43797.

24. Simões JB, Araújo CJ. Nickel–titanium shape memory alloy mechanical components produced by investment casting. *Journal of Intelligent Material Systems and Structure*. 2018;29(19):3748-3757.

25. Elahinia M. *Shape Memory Alloy Actuators: Design, Fabrication and Experimental Evaluation*. Hoboken: Wiley; 2016.

26. de Araújo CJ, Gomes AAC, Silva JA, Cavalcanti AJT, Reis RPB, Gonzalez CH. Fabrication of shape memory alloy using the plasma skull push-pull process. *Journal of Materials Processing Technology*. 2009;209(7):3657-3664.